Isoscalar spin observables in quasielastic deuteron scattering

M. D. Holcomb* and R. J. Peterson
Nuclear Physics Laboratory, University of Colorado, Boulder, Colorado 80309-0446

E. Tomasi-Gustafsson
Laboratoire National Saturne, CEN Saclay, F-91191 France

M. Morlet, J. Guillot, H. Langevin-Joliot, L. Rosier, and A. Willis
Institut de Physique Nucleaire, Orsay, F-91406, France

B. N. Johnson
Department of Physics and Astronomy, University of South Carolina, Columbia, South Carolina 29208
(Received 3 November 1997)

Inelastic scattering of 600 MeV vector and tensor polarized deuterons has been carried out at energy losses corresponding to quasielastic, incoherent scattering from individual nucleons in targets of CH_2, CD_2, C, Ca, and Pb at fixed momentum transfers of 345 and 500 MeV/c. Vector (A_y) and tensor (A_{yy}) analyzing powers were measured, and the vector polarizations $P_{y'}$ of the scattered deuterons were determined by the polarimeter POMME. These observables were combined to determine the vector spin transfer coefficients $K_y^{y'}$ for the deuterons and several signatures for spin transfer probabilities across the quasielastic spectra. [S0556-2813(98)03304-4]

PACS number(s): 25.45.De, 24.70.+s, 25.10.+s

I. INTRODUCTION

Since the π meson is expected to generate strong correlations among the nucleons in a complex nucleus, scattering specific to the quantum numbers of the π meson has been studied under kinematic conditions such that the projectile has interacted incoherently with individual nucleons in complex targets as they interact with their nuclear host. The largest body of data arises from the isovector $(\vec{p},\vec{n})$ reaction [1,2]. Knowledge of the proton beam polarization and measurement of the polarization of the outgoing neutrons can be combined to yield knowledge of both the longitudinal spin scattering (with an interaction proportional to $\vec{\sigma}\cdot\vec{q}$) and the transverse scattering (proportional to $\vec{\sigma}\times\vec{q}$). Here, the spin projection of the struck nucleon is $\vec{\sigma}$ and $\vec{q}$ is the three-momentum transfer. Since the charge exchange reaction is explicitly isovector, the quantum numbers of the means to transfer the momentum correspond to the pion interactions of the struck nucleon in the longitudinal channel, and most simply to the ρ meson interactions in the transverse channel. The transverse channel has also been the subject of extensive quasielastic scattering studies with electron beams, also primarily isovector [3]. A review of the specific transition quantum numbers probed by a variety of simple projectiles is found in Ref. [4], and a recent review of the nuclear spin responses to the scattering of polarized protons and deuterons is found in Ref. [5].

With two possible isospin channels and three possible spin channels (transverse, longitudinal, and nonspin), interactions of a projectile with a single nucleon include six possible combinations. It is the purpose of this study to measure quasielastic observables in strictly isoscalar spin channels by the scattering of deuterons. The lightest single mesons that would contribute to isoscalar correlations would be the η in the longitudinal interaction and the ω in the transverse, as determined by their quantum numbers. The multiple exchange of mesons can also provide these correlations. Although the isoscalar channel also contributes to the scattering of protons, at the beam energies needed to achieve quasielastic kinematics these data are dominated by the isovector interactions of the proton beam [6–8]. These experiments found that spin transfer is enhanced at high excitations, in contrast to its suppression at low excitations.

Our experiment measured the scattering of 600 MeV polarized deuterons at angles and energy losses corresponding to scattering from free nucleons, with energy losses near $\omega = q^2/2m$, with m the nucleon mass. Values of the laboratory-frame three-momentum transfer q to the deuteron were selected to be 345 and 500 MeV/c, or 1.75 and 2.5 fm^{-1}, to match recent data from the (p,n) reaction [2] and from the (p,p') reaction [6]. Targets were selected to be CH_2, CD_2, C, Ca, and Pb to match the isovector experiments. Knowledge of both the vector (A_y) and tensor (A_{yy}) analyzing powers of the deuterons, of the vector spin transfer coefficients $K_y^{y'}$, and of the absolute cross sections would be sufficient to determine all of the isoscalar spin responses of the targets if the conditions of the plane wave impulse approximation were met. The relations that determine the scattering observables have been given by Suzuki [9,10] and are described in the Appendix.

Since our experiment measured only the spin observables, without absolute cross sections, we are not able to invert the expressions of Suzuki to find the nuclear isoscalar responses. Our data trace out the evolution of the spin observables across the region of the quasifree peak, and compare those

*Present address: Johnson-Matthey Semiconducors, Chippewa Falls, WI 54729.

TABLE I. Polarization states of the deuteron beams and their theoretical maxima.

State	1	2	3	4	5	6	7	8
P_y	0	$-2/3$	$+2/3$	0	$+1/3$	$-1/3$	$+1/3$	$-1/3$
P_{yy}	0	0	0	0	$+1$	$+1$	-1	-1

for a sample of complex targets to those for free protons. Any calculated isoscalar nuclear responses may then be used in the expressions of Suzuki for comparison to data from the experiment.

These methods to determine and interpret deuteron spin observables in elastic scattering from complex nuclei have previously been applied to excitations of discrete states and the low-lying continuum, where the quantum numbers of the coherent nuclear states are known [11–14]. Those studies at low momentum transfer allow us to compare our data to results for coherent states of specific and known spin structure. Quasielastic scattering proceeds through the incoherent sum of allowed quantum numbers, as if the target were a free nucleon, and is the incoherent sum of all contributing multipoles.

II. EXPERIMENT

Our experiment was carried out at the Laboratoire National Saturne. The polarized deuteron beams originated in the atomic beam source HYPERION [15], with vector beam polarizations P_y and tensor beam polarizations P_{yy} listed in Table I with their maximum allowed values. Beam polarization states were changed for each synchrotron cycle in two separate run modes. The two-state beam alternated between states 2 and 3, and the four-state beam cycled through states 5, 6, 7, and 8. The two-state beam was used to obtain accurate vector analyzing powers and to measure vector spin transfer coefficients. The four-state beam was used to determine tensor analyzing powers and to provide an independent check of the vector analyzing powers.

Vector (P_y) and tensor (P_{yy}) beam polarizations were measured several times during the experiment by a polarimeter near the source, using the $^2\mathrm{H}(d,p)^3\mathrm{H}$ reaction [15]. Weighted averages of the beam polarizations used during the experiment were

$$\text{two-state}\quad P_y = 0.603 \pm 0.009,$$

$$\text{four-state}\quad P_y = -0.317 \pm 0.009,$$

$$P_{yy} = 0.356 \pm 0.051\ \ (\text{for}\ \ q = 345\ \ \text{MeV}/c)$$

$$= 0.837 \pm 0.021\ \ (\text{for}\ \ q = 500\ \ \text{MeV}/c).$$

The tensor polarization was anomalously low for our runs at 345 MeV/c. An additional uncertainty of $\pm 2.5\%$ arises from the calibration of the low-energy polarimeter [15]. These deuterons were accelerated to 600 MeV in the storage ring-booster MIMAS and the synchrotron SATURNE. It has been shown that the intitial beam polarization is maintained in the acceleration up to 2.3 GeV [16].

Scattering targets were natural isotopic mixtures of Pb, Ca, C, and CH_2, and a highly enriched CD_2 foil. The Ca target was clad in thin aluminum foil. Targets were up to 200 mg/cm^2 thick, and their thicknesses were known to an accuracy of 1%.

Scattered deuterons were detected in the magnetic spectrometer SPES1. Essentially no counts were seen from runs without scattering targets. Since the momentum acceptance of SPES1 is only 4%, up to five field settings were used to obtain overlapping spectra across the wide quasielastic region. The scattering angle was changed for each momentum setting to maintain a fixed momentum transfer at the center of the spectrometer acceptance, from 9.8° to 12.1° for $q = 345$ MeV/c and from 15.8° to 18.0° for $q = 500$ MeV/c. All events in the 2.7° angular acceptance were binned together. An unnormalized spectrum for scattering from carbon is shown in Fig. 1 [17], at a momentum transfer of 500 MeV/c, using an empirical acceptance function for SPES1 derived from forcing the spectra for lead to be continuous. Counts from five spectrometer settings are superimposed for this spectrum. The curve shown is calculated for the quasielastic scattering from a gas of nucleons with a Fermi momentum of 221 MeV/c for carbon, as determined from electron scattering [18]. The region of the spectrum that we cover includes most of the quasielastic region. The narrower quasielastic peak at $q = 345$ MeV/c is even more completely covered by our data. The quasielastic peak for deuterium is expected to be narrower, with a full width at half maximum of about 40 MeV observed by electron scattering at 500 MeV/c [19]. Isovector spectra of the nuclear continuum are complicated by the presence of counts due to pion production, but this feature will not be present in the isoscalar deuteron scattering, which would then look more similar to the quasielastic spectra for the charge channel in electron scattering [3].

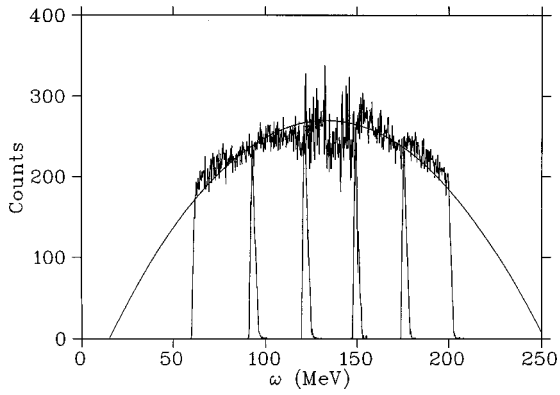

FIG. 1. A missing energy spectrum of 600 MeV deuterons scattered from carbon at laboratory angles from 15.8 to 18.0°, so as to maintain a fixed momentum transfer of 500 MeV/c to the scattered deuteron. Five overlapping spectra are shown, using a relative acceptance function taken from a demand that the continuum spectrum for scattering from our lead target be smooth. The curve shows the expected cross section for quasielastic scattering from a Fermi gas with $k_F = 221$ MeV/c.

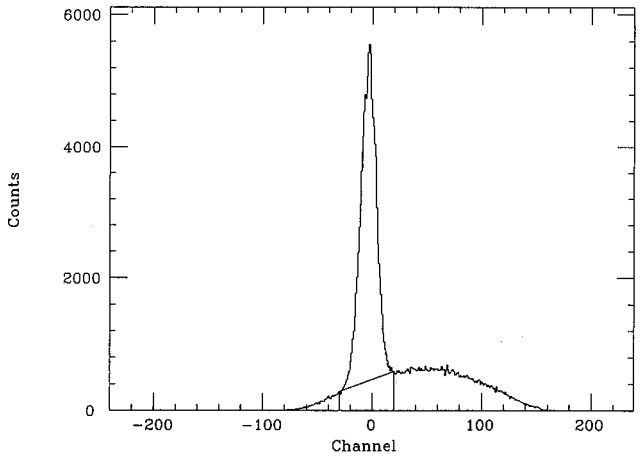

FIG. 2. A missing mass spectrum of two-state 600 MeV deuterons scattered from a CH_2 target at 17.3°, without acceptance corrections. The sharp peak for scattering from protons is superimposed on the carbon quasielastic scattering spectrum at this momentum transfer of 500 MeV/c.

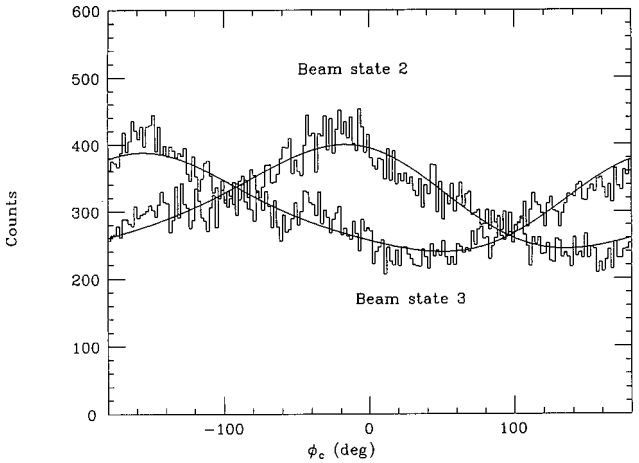

FIG. 3. Second-scattering events measured by the polarimeter POMME are shown for azimuthal angles about the direction of the scattered particle for two vector beam polarization states. Counts from the full momentum acceptance of SPES1 and for its full angular acceptance target and scattering angle were added to improve the statistical accuracy. The curves show fits with the form of Eq. (1). Similar data for each 5 MeV bin in ω and each 1° bin in θ_c were fit to determine the coefficients a_1 used in Eq. (2) across the full range of missing energies ω.

The relative intensity of the beam for each target was monitored by plastic scintillator telescopes viewing the beam spot. Monitor M was in the y-z scattering plane, 60° above the x-z scattering plane, and insensitive to the vector polarization of the beam. Monitor N was in the x-z scattering plane, at 45° from the beam direction. The counts the monitors observed depended on the beam polarization, the target thickness, and the target analyzing power for the products each monitor observes. No Faraday cup was available for absolute beam intensity determinations.

Vector polarizations $P_{y'}$ of the outgoing deuterons were determined with the polarimeter POMME attached to the rear of SPES1 [20]. With scattering in the horizontal plane, a horizontal bend, and horizontal dispersion, SPES1 does not precess the normal component of the deuteron spin measured by POMME. The figure of merit for this polarimeter is large for deuterons corresponding to quasielastic scattering at $q = 345$ and 500 MeV/c for the 600 MeV incident beam energy, and its vector analyzing power iT_{11} is known [20]. Two thicknesses of the carbon and iron absorbers in the polarimeter were used to maintain a high figure of merit as the spectra included a wide range of scattered deuteron energies. About 90% of the deuterons scatter by less than 5° in the carbon second scattering planes of POMME, and these carry little polarization information. A fast on-line software system in this experiment rejected events that scattered in POMME by less than about 2°.

During data analysis the checks and tests described in [12,13] were satisfactorily carried out in a series of replays. A typical missing mass histogram is shown in Fig. 2, for the events observed in scattering from the CH_2 target at 17.3°, using the two-state beam. The sharp peak is from the free protons in the sample, and the broad continuum arises from the quasielastic scattering from carbon, uncorrected for the acceptance of the spectrometer. The observed width of 8 MeV for the proton peak is dominated by incomplete compensation of kinematic effects in the energy-loss spectrometer SPES1, and may also be taken to be the resolution of our quasifree spectra.

Vector polarizations for scattered deuterons were determined from the azimuthal distribution of events in POMME. A sample distribution at 500 MeV/c is shown in Fig. 3. We fit these ϕ distributions for each POMME scattering angle θ_c by the form

$$N(\theta_c,\phi_c) = a_0 + a_1\cos\phi_c + a_2\cos 2\phi_c + b_1\sin\phi_c + b_2\sin 2\phi_c, \quad (1)$$

where the coeffieients will depend upon θ_c. The coefficients b_1 and b_2 were small, relative to a_0, a_1, and a_2, for all values of θ_c beyond the 2.5° software cut.

The analyzing power A_y of POMME depends upon the deuteron momentum, and has been made available as the coefficient $iT_{11}(\theta_c)$ [20]. The deuteron momentum at the point of the analyzing scattering event was estimated to be that at the middle of the carbon scattering plane where the scattering occurred. The polarization of the scattered deuteron is then determined from

$$P_{y'} = \frac{1}{\sqrt{3}} \quad \frac{a_1(\theta_c)}{iT_{11}(\theta_c)}. \quad (2)$$

$P_{y'}$ is independent of θ_c but is determined by a series of analyses in θ_c from 2.5° to 10°. A weighted average of polarizations was formed for each beam state during a run, and these averages were combined for runs at the same momentum setting for each target to form the final result. The uncertainties in the fitted coefficients a_1 and in the published values of iT_{11} were used to determine the final uncertainty in $P_{y'}$.

III. DATA ANALYSIS

It may not be safe to assume that each synchrotron spill carried exactly the same number of polarized deuterons, and

we must know how many beam particles were in each state in order to determine analyzing powers. We used a numerical fitting procedure to estimate the analyzing power for each target at each of the monitor angles to determine the correct beam fractions for each run. An attempt to determine these by algebraic methods encountered dangerously unstable uncertainties due to the differences of very large numbers.

Predicted numbers of counts in monitors M and N for each beam state p are given by

$$
\begin{aligned}
M_5 &= f_5(1+\tfrac{1}{2}P_{yy}A_{yy}^M)(I\sigma_{M0}/K_{MT}),\\
M_6 &= f_6(1+\tfrac{1}{2}P_{yy}A_{yy}^M)(I\sigma_{M0}/K_{MT}),\\
M_7 &= f_7(1-\tfrac{1}{2}P_{yy}A_{yy}^M)(I\sigma_{M0}/K_{MT}),\\
M_8 &= f_8(1-\tfrac{1}{2}P_{yy}A_{yy}^M)(I\sigma_{M0}/K_{MT}),\\
N_5 &= f_5(1-\tfrac{3}{2}P_yA_y^N+\tfrac{1}{2}P_{yy}A_{yy}^N)(I\sigma_{N0}/K_{NT}),\\
N_6 &= f_6(1+\tfrac{3}{2}P_yA_y^N+\tfrac{1}{2}P_{yy}A_{yy}^N)(I\sigma_{N0}/K_{NT}),\\
N_7 &= f_7(1-\tfrac{3}{2}P_yA_y^N-\tfrac{1}{2}P_{yy}A_{yy}^N)(I\sigma_{N0}/K_{NT}),\\
N_8 &= f_8(1+\tfrac{3}{2}P_yA_y^N+\tfrac{1}{2}P_{yy}A_{yy}^N)(I\sigma_{N0}/K_{NT}),
\end{aligned}
\tag{3}
$$

where K denotes a combination of monitor solid angle and target thickness contributions, f_p is the fractional beam intensity in each state, A^N and A^M are the analyzing powers of each target at the monitor angles, where cross sections are σ_0, and I is the beam intensity. From reasonable initial estimates for the terms on the right side of this equation, the predicted numbers of counts were compared to the actual values M_p and N_p. Nine unknowns were varied among eight equations to achieve the best value of χ^2. The sensitivity of the result to the parameters around the χ^2 minimum yielded a stable uncertainty for each determination. This stability may be traced to the small values of the target analyzing powers A^M and A^N at the monitor angles. The beam fractions in each spin state were very near the simplest expectation of 1/2 in each of states 2 and 3 and 1/4 in each of states 5, 6, 7, and 8.

This procedure was carried out for each run for each 5 MeV wide bin in deuteron missing energy, using the average beam intensities in each state for each run. Analyzing powers for the two-state beam were determined by

$$A_y=\frac{2}{3P_y}\frac{f_2S_3-f_3S_2}{f_2S_3+f_3S_2}, \tag{4}$$

and for the four-state beam by

$$A_y=\frac{2}{3P_y}\frac{S_5/f_5-S_6/f_6+S_7/f_7-S_8/f_8}{S_5/f_5+S_6/f_6+S_7/f_7+S_8/f_8}, \tag{5}$$

$$A_{yy}=\frac{2}{P_{yy}}\frac{S_5/f_5+S_6/f_6-S_7/f_7-S_8/f_8}{S_5/f_5+S_6/f_6+S_7/f_7+S_8/f_8}, \tag{6}$$

using the beam fractions f_p and the good spectrometer events S_p for each state. Uncertainties arise largely from the statistical uncertainties of S_p. Overlapping regions of the missing mass spectra were suitably averaged. Missing mass distributions of spin observables for H and D were determined by appropriate subtractions using the carbon target.

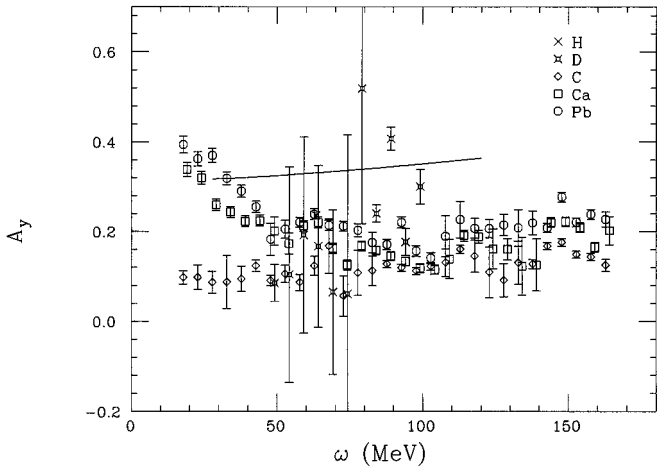

FIG. 4. Vector analyzing powers A_y determined for the scattering of 600 MeV four-state deuteron beams are shown for all targets at a momentum transfer of 345 MeV/c. For reference, note the free proton datum at $\omega=62$ MeV and $A_y=0.236$ (0.008) and the curve taken from 300 MeV isoscalar nucleon-nucleon scattering.

IV. RESULTS

Vector analyzing powers A_y for all targets are shown in Fig. 4, using the four-state beam, and in Fig. 5, using the two-state beam, at 345 MeV/c. The energy scale is the laboratory-frame energy loss of the scattered deuterons. Elastic scattering from D would be at $\omega=31$ MeV, while elastic scattering peaks for C, Ca, and Pb would be at $\omega=5$, 2, and 0 MeV, respectively. Scattering from free protons puts a single point at $\omega=62$ MeV on this scale. These two indepen-

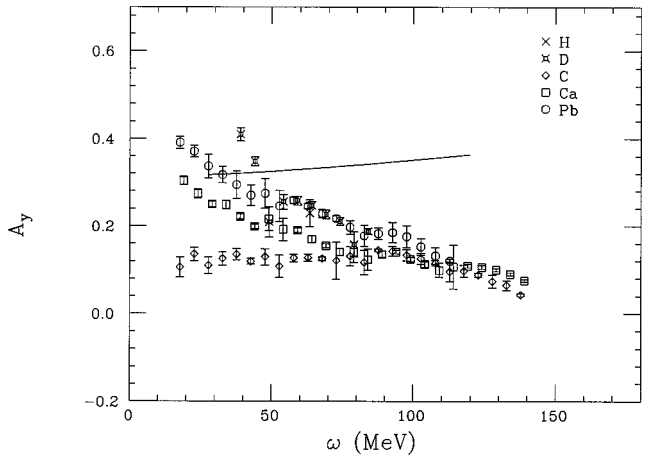

FIG. 5. Vector analyzing powers A_y determined for the scattering of 600 MeV two-state deuteron beams are shown for all targets at a momentum transfer of 345 MeV/c. For reference, note the free proton datum at $\omega=62$ MeV and $A_y=0.229$ (0.031) and the curve taken from 300 MeV isoscalar nucleon-nucleon scattering. The statistical accuracy of these data is better than those shown in Fig. 4 because of the higher vector polarization and the longer running periods used for the two-state beam.

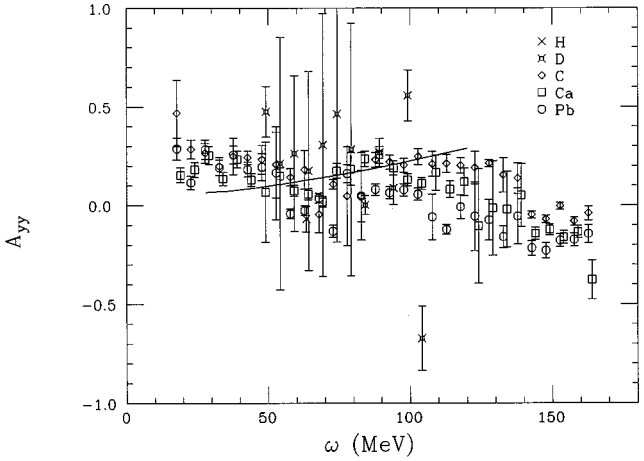

FIG. 6. Tensor analyzing powers A_{yy} determined for the scattering of 600 MeV four-state deuteron beams are shown for all targets at a momentum transfer of 345 MeV/c. For reference, note the datum for free protons at $\omega = 62$ MeV and $A_y = -0.069$ (0.06) and the curve from free isoscalar scattering.

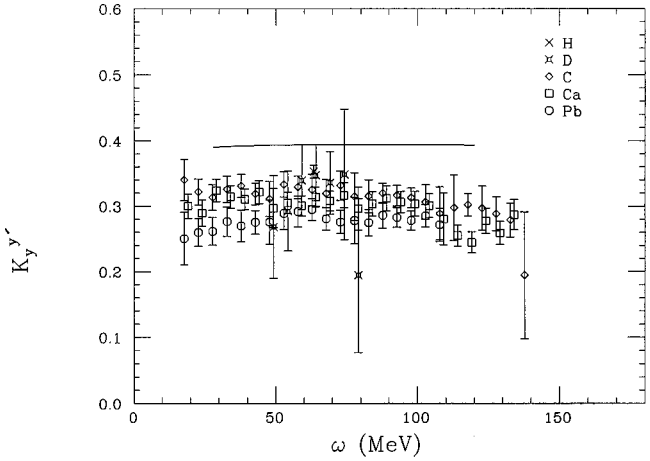

FIG. 8. Vector spin transfer coefficients $K_y^{y'}$ for the scattering of 600 MeV vector polarized deuterons from all targets at a momentum transfer of 345 MeV/c are shown. For reference, note the datum for free protons at $\omega = 62$ MeV and $K_y^{y'} = 0.35$ (0.01) and the curve from free isoscalar scattering.

dent determinations of A_y agree well, except possibly at the largest energy transfers. One more spectrometer setting was taken with the four-state beam than with the two-state beam. Reduced χ^2 values for the agreement between the two-state and four-state measurements of A_y are 1.3 for deuterium, 2.3 for carbon, 2.0 for calcium, and 0.8 for lead, neglecting systematic uncertainties.

It is remarkable to note how closely the data from all targets are in agreement across the quasifree peak, which would have a parabolic shape centered near 62 MeV and with a full width of 147 MeV for a gas of nucleons with Fermi momentum 200 MeV/c. The data shown at 345 MeV/c span this entire range.

Tensor analyzing powers A_{yy} for all targets at $q = 345$ MeV/c are shown in Fig. 6 and the polarizations $P_{y'}$ of deuterons scattered from all targets are shown in Fig. 7 at this momentum transfer. The upper band is obtained from beam state 2 and the lower from beam state 3. Since the initial beam polarizations were about 61%, these scattered polarizations show that the reaction depolarized the beam, and not symmetrically.

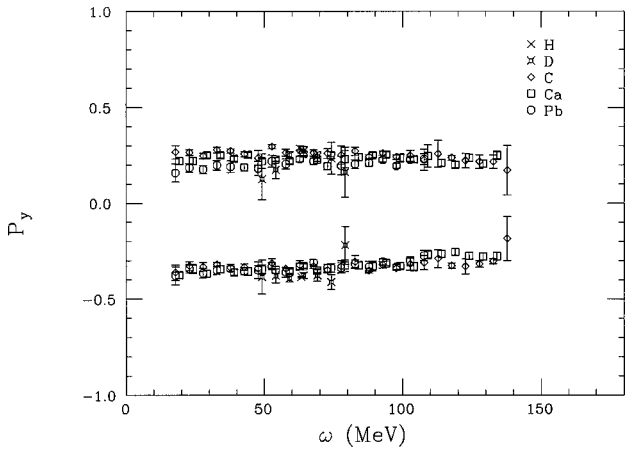

FIG. 7. Vector polarizations $P_{y'}$ measured for the scattering from all targets of vector polarized 600 MeV deuterons at momentum transfers of 345 MeV/c. The upper band is for beam state 2 and the lower band is for beam state 3, each with about 61% beam polarization. Proton data are at $\omega = 62$ MeV and $P_{y'} = 0.280$ (0.004) and -0.386 (0.004).

Spin transfer coefficients $K_y^{y'}$ were computed from

$$K_y^{y'} = \frac{1}{3P_y}[P_{y'}(2)(1+\tfrac{3}{2}P_yA_y) - P_{y'}(3)(1-\tfrac{3}{2}P_yA_y)], \tag{7}$$

and are plotted in Fig. 8. The curves shown for these spin observables are for scattering 300 MeV nucleons from free nucleons, in the isoscalar channel only, at the angles used to maintain the fixed momentum transfer. These observables were calculated from a phase shift analysis of free nucleon-nucleon scattering [21], and are near the observed 600 MeV deuteron data for free protons in our CH_2 target at 345 MeV/c.

At $q = 500$ MeV/c, vector analyzing powers A_y are plotted for all targets in Fig. 9 using the four-state beam, and in Fig. 10 using the two-state beam. The reduced χ^2 for agreement between the data from the two beam states are 3.6, 1.5, and 1.4 for C, Ca, and Pb, respectively. Scattering from free protons yields a single datum at $\omega = 132$ MeV, and a Fermi gas parabola of quasifree scattering would extend from 30 to 230 MeV of energy loss. These data are in agreement for the two beam states for each target nucleus, although two more spectrometer settings were used to gain the wider coverage seen with the four-state beam. We note a steady upward progression of this observable as the target mass increases.

The tensor analyzing powers A_{yy} at $q = 500$ MeV/c are shown in Fig. 11. The datum for free protons at 132 MeV and the narrow distribution of counts for the deuterium target are notable above the uniform trend seen for the other targets. Polarizations $P_{y'}$ for scattered deuterons are shown at 500 MeV/c in Fig. 12 and the vector spin transfer coefficients $K_y^{y'}$ are shown in Fig. 13. These observables vary little from target to target. Elastic scattering peaks for D, C, Ca,

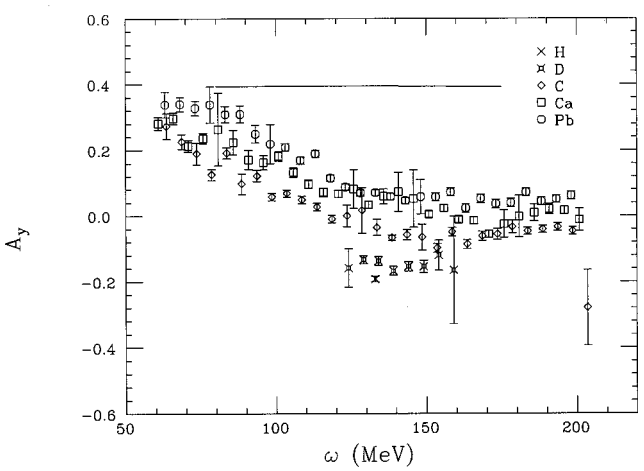

FIG. 9. Vector analyzing powers A_y are shown for all targets for the scattering of 600 MeV four-state beam at a momentum transfer of 500 MeV/c. For reference, note the datum for free protons at $\omega=132$ MeV and $A_y=-0.208$ (0.004) and the curve from free isoscalar scattering.

and Pb would be found at $\omega=62$, 11, 3, and 1 MeV, respectively, for these spectra at $q=500$ MeV/c, using our scale of energy loss to the projectile.

In contrast to the case at 345 MeV/c, the curves shown for the free spin observables [21] at 500 MeV/c are not near the proton data from our CH_2 target. By this higher momentum transfer the D state of the deuteron projectile has a large influence not included in the estimate made through that simplest approximation.

Signatures for spin transfer have been derived by Suzuki and by Morlet. The combination S_y^d was shown by Morlet [12] to be the probability of transferring one unit of the y component of the deuteron total spin, computed by

$$S_y^d=\frac{4}{3}+\frac{2}{3}A_{yy}-2K_y^{y'}. \tag{8}$$

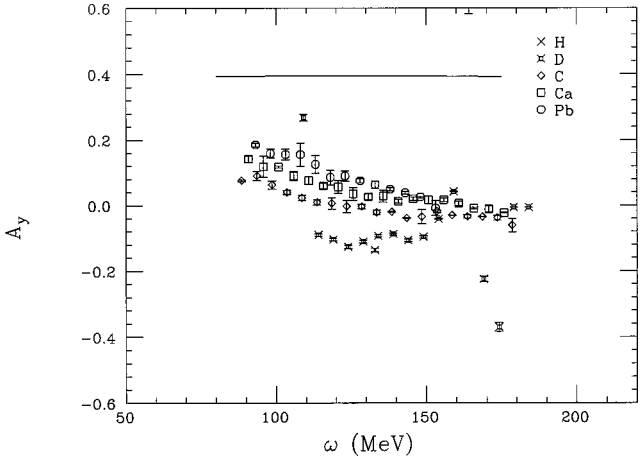

FIG. 10. Vector analyzing powers A_y are shown for all targets for the scattering of 600 MeV two-state beam at a momentum transfer of 500 MeV/c. For reference, note the datum for free protons at $\omega=132$ MeV and $A_y=-0.153$ (0.03) and the curve from free isoscalar scattering. The statistical accuracy of these data is better than seen in Fig. 9 because of the higher vector polarization and longer running time with the two-state beam.

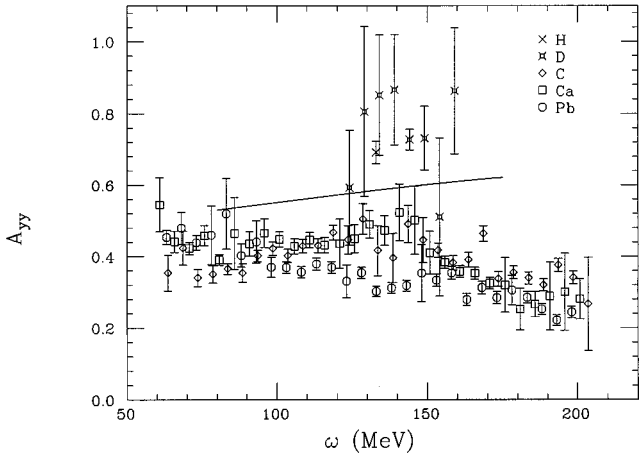

FIG. 11. Tensor analyzing powers A_{yy} are shown for all targets for the scattering of 600 MeV four-state beam at the momentum transfer of 500 MeV/c. For reference, note the datum for free protons at $\omega=132$ MeV and $A_{yy}=0.69$ (0.03) and the curve from free isoscalar scattering.

This spin transfer signature has been measured to be 0.38 (0.03) [13] and 0.44 (0.03) [22] for the $0^+\rightarrow1^+$ 12.7 MeV transition in ^{12}C at $q=92$ MeV/c. This signature has been shown to be effective in the selection of $\Delta S=1$ transitions and to be near zero for nonspin transitions [11]. Values of this quasifree observable are shown in Fig. 14 at 345 MeV/c and in Fig. 15 at 500 MeV/c. Results for all complex targets are a bit above the proton datum at 345 MeV/c, but nearly atop the proton datum at 500 MeV/c. The validity of this S_y^d to determine ''spin flip'' has only been demonstrated at angles below 10° [13], whereas the data we treat are from larger scattering angles. These data also exceed the values of S_y^d computed from free isoscalar N-N observables.

The signature σ_1 is defined by Suzuki [9] to be

$$\sigma_1=2+2A_{yy}-3K_y^{y'}, \tag{9}$$

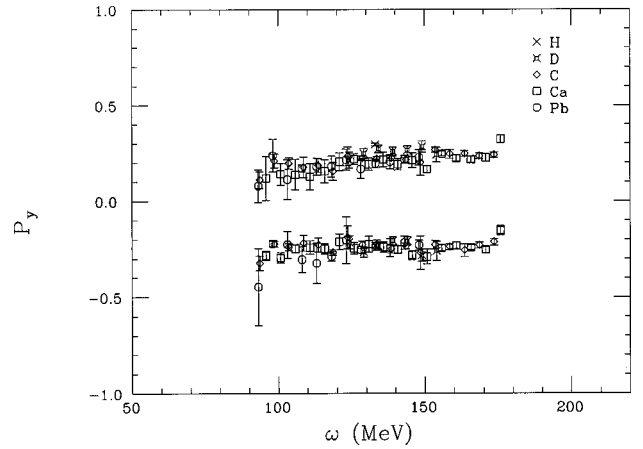

FIG. 12. Vector polarizations $P_{y'}$ measured by POMME are shown for all targets for the scattering of 600 MeV vector polarized deuterons at a momentum transfer of 500 MeV/c. The upper band is for beam state 2 and the lower band is for beam state 3; each state had a vector beam polarization near 61%. Proton data are at $\omega=132$ MeV and $P_{y'}=0.294$ (0.007) and -0.234 (0.008).

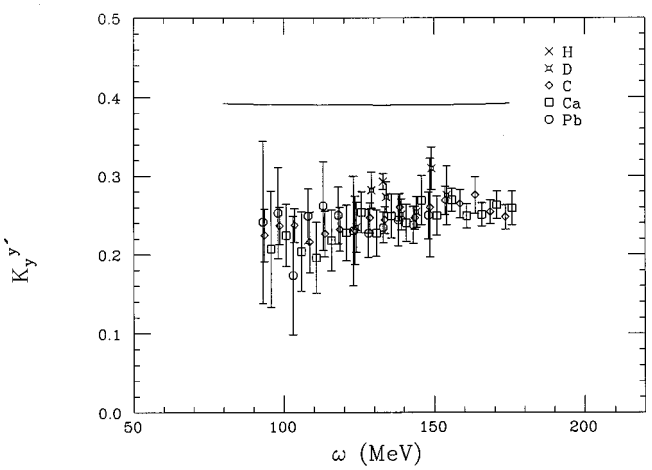

FIG. 13. Vector spin transfer coefficients $K_y^{y'}$ are shown for all targets for the scattering of 600 MeV vector polarized deuterons at a momentum transfer of 500 MeV/c. For reference, note the datum for free protons at $\omega = 132$ MeV and $K_y^{y'} = 0.293$ (0.010) and the curve from free isoscalar scattering.

and represents the probability to transfer one unit of total spin magnitude to the projectile; σ_1 is not zero for a $\Delta S = 0$ transition. This signature may be thought of as the ''spin flip'' probability, although it often exceeds unity in our data. For the 12.7 MeV $0^+ \rightarrow 1^+$ transition in ^{12}C this signature σ_1 is 0.58 (0.06) at 92 MeV/c, from the data in Ref. [22]. Quasifree data for σ_1 are shown at 345 MeV/c in Fig. 16 and at 500 MeV/c in Fig. 17. Similar to the observable S_y^d, this signature shows all complex target data to be slightly above the proton datum at 345 MeV/c and all targets are very similar at 500 MeV/c. The 500 MeV/c data are near the values computed for free isoscalar N-N scattering.

These signatures are discussed in more detail, including the role of tensor spin transfer observables, in Ref. [22].

V. DISCUSSION

The isoscalar correlations in complex nuclei brought about by nuclear inteactions have been considered in several

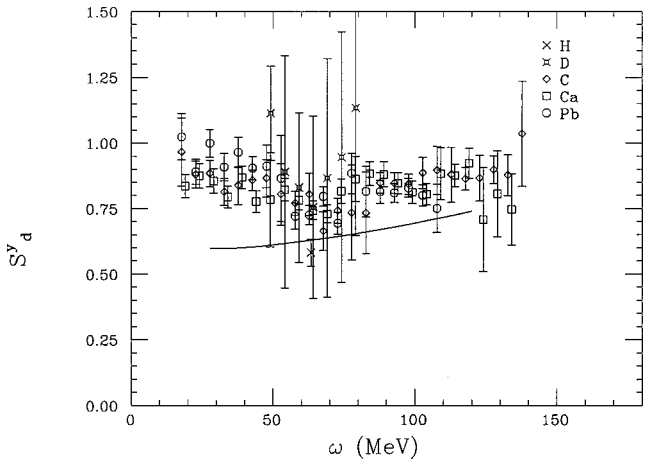

FIG. 14. Spin signatures S_y^d are shown for all targets at a momentum transfer of 345 MeV/c. For reference, note the datum for free protons at $\omega = 62$ MeV and $S_y^d = 0.58$ (0.05) and the curve from free isoscalar scattering.

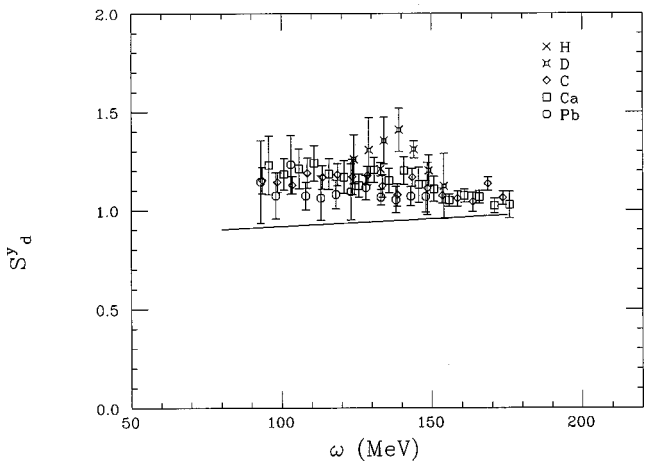

FIG. 15. Spin signatures S_y^d are shown for all targets at a momentum transfer of 500 MeV/c. For reference, note the datum for free protons at $\omega = 132$ MeV and $S_y^d = 1.21$ (0.03) and the curve from free isoscalar scattering.

sets of calculations. The lightest single mesons that could be exchanged to carry the relevant quantum numbers would be the σ (nonspin), η (spin longitudinal), and ω (spin transverse). Because the η, in particular, is known to have only fairly weak couplings to nucleons [23], these calculations have not been restricted to single-meson exchange contributions. It has been shown, for instance, that the exchange portion of the tensor interaction brought about by pion exchange can have strong correlating effects in isoscalar channels [24–28]. These quench the isoscalar longitudinal quasielastic spin response relative to the free and enhance the transverse [25,26]. These behaviors are just opposite to the features expected in the isovector channels. Both spin responses are harder than the uncorrelated case, with quasielastic peaks at larger energy losses ω than found for free scattering. Ground state correlations contribute strongly to this hardening [26]. The binding energy of the struck nucleon does not influence the energy loss ω of the scattered projectile [29].

All of these calculations have been carried out at the densities of complete nuclei. Our deuteron scattering probe is

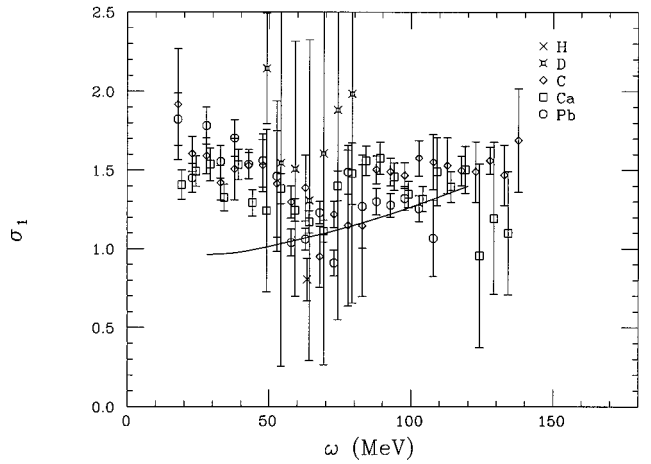

FIG. 16. Spin signatures σ_1 are shown for all targets at a momentum transfer of 345 MeV/c. For reference, note the datum for free protons at $\omega = 62$ MeV and $\sigma_1 = 0.80$ (0.14) and the curve from free isoscalar scattering.

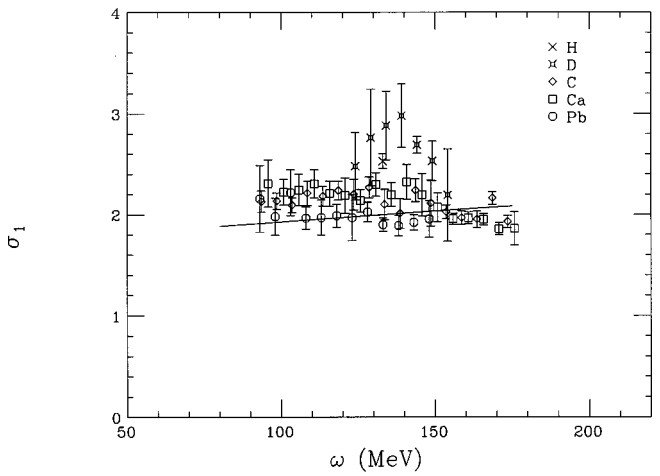

FIG. 17. Spin signatures σ_1 are shown for all targets at a momentum transfer of 500 MeV/c. For reference, note the datum for free protons at $\omega=132$ MeV and $\sigma_1=2.53$ (0.07) and the curve from free isoscalar scattering.

very strongly absorbed by nuclei, and the surviving quasielastic events come only from surface scattering. We have used the known deuteron-nucleon total cross section of 80 mb [30] and the Glauber approximation to estimate the number of nucleons $A_{\rm eff}$ sensed by the quasielastic reaction, using the methods described in Ref. [31]. The resulting $A_{\rm eff}$ is given by $A_{\rm eff}=0.74\ A^{0.30}$. For Pb, we are scattering only from fewer than four nucleons, corresponding to those nucleons found outwards from where the density is only 4% of the central density. For Ca and C, we sense densities only outwards from 6 and 14 % of the central values, respectively. Correlations at these low densities might very well be weaker than those at full density.

Another view of the effects of transverse isoscalar interactions is found in the systematic quenching of stretched magnetic excitations noted by high resolution pion inelastic scattering [32]. These studies are carried out at momentum transfers near 345 MeV/c, with the two pion charge states giving accurate decompositions of isoscalar and isovector amplitudes. The spin zero of the pion projectile precludes coupling to spin longitudinal modes. These pion scattering data find that the summed isoscalar magnetic strength is much less than the isovector strength for these simple nuclear states, and much less than is computed even in large basis shell model calculations. For this reason, and because of what has been learned from basic theory, we anticipate quite different trends in our isoscalar scattering than those seen in the (p,n) experiments.

We will first use the isoscalar data for our range of targets to track changes in each spin observable. Vector analyzing powers A_y at 345 MeV/c in Figs. 4 and 5 are near the free scattering values of 0.236 (0.008) and 0.229 (0.031) at $\omega=62$ MeV at the centers of the quasielastic peaks for D, Pb, and Ca. Relative to free scattering this spin observable is enhanced at lower excitations in the largest nuclei, in what appears to be a systematic fashion. Data for carbon are flat across the entire spectrum.

This tendency is maintained at 500 MeV/c, as seen in Figs. 9 and 10. A_y data for all targets are more strongly positive for all targets than are the data for protons of $A_y=-0.280$ (0.004) and -0.153 (0.03) at $\omega=132$ MeV. There is an upward slope towards lower energy losses, and this is stronger for the heavier targets.

Tensor analyzing power (A_{yy}) data shown in Fig. 6 at 345 MeV/c and in Fig. 11 at 500 MeV/c show no strong dependence upon ω for the complex targets at either momentum transfer. At 345 MeV/c all data are very near the free proton point at $A_{yy}=-0.069$ (0.06). At 500 MeV/c, the deuterium data are quite near the datum for free protons at $A_{yy}=0.69$ (0.03), but all other targets show consistently lower values. Coherent nuclear states excited by 400 MeV deuterons scattering at lower momentum transfers show values of A_y and A_{yy} that are positive for states of natural parity and very small for states of unnatural parity that require spin transfer [16].

Scattered deuteron polarizations $P_{y'}$ show no dependence upon the target or the energy transfer ω in the spectra of Fig. 7 at 345 MeV/c or Fig. 12 at 500 MeV/c. Within the larger uncertainties, this is also true of the vector spin transfer probabilities $K_y^{y'}$, seen in Fig. 8 at 345 MeV/c or in Fig. 13 at 500 MeV/c.

Spin transfer probabilities at 345 MeV/c, either S_y^d in Fig. 14 or σ_1 in Fig. 16, show a dip for all complex targets just at the free scattering value of $\omega=62$ MeV, with a width of about 20 MeV. This dip brings these observables closer to the free proton scattering data than is seen elsewhere in the continuum spectra. The full width at half maximum for scattering from a Fermi gas with $k_F=200$ MeV/c would be 104 MeV at this momentum transfer, much broader than the structure noted in the data. Both spin signatures are structureless and target-independent at 500 MeV/c in Fig. 15 and Fig. 17, and only a bit below the free proton datum. The narrow deuteron peak is, however, actually somewhat above the free proton result. These free and quasifree spin signatures are far greater than the values of 0.4 for S_y^d and 0.58 for σ_1 for the coherent spin excitation of the 12.7 MeV state in ^{12}C at 92 MeV/c [13,22].

One of the greatest expected differences that could be expected for the range of targets studied would be the role of distortions due to the very strong influence of the nucleus upon the deuterons. These distortions would be less dependent upon the energy loss ω for a given target. What we see, however, is only a minor target dependence for only one observable (A_y), but a more persistent trend across the energy loss spectrum. Since the deuterons scattered at each angle with the proper energy are those corresponding to single quasielastic scattering, it is not suprising that there is little target dependence of the distortions, since those distortions primarily determine only the rarity of the single scattering events seen. The small fraction of the deuteron-nucleon total cross section that occurs elastically makes it unlikely that an outgoing deuteron has participated in more than one elastic event within the nucleus.

Our data for these spin observables do not permit inversion to determine the isoscalar spin responses, which are the quantities computed in such efforts as those of Refs. [24–28]. If, however, theory provides a full set of the three isoscalar responses, the Appendix shows how these might be used in the plane-wave impulse approximation to compute

TABLE II. Deuteron-nucleon form factors from Eq. (A9) and isoscalar nucleon-nucleon amplitudes are given in this table. These are generated at exactly the angles needed for free scattering. Deuteron form factors are from the average of five theoretical results described in the text, with an uncertainty given by their scatter. Complex nucleon-nucleon amplitudes in fm are from the SM95 solution of SAID for isoscalar *N*-*N* scattering at 300 MeV [21].

q (MeV/c)	g_C	g_Q	g_S	g_L	
345	0.3188(0.0075)	−0.0459(0.0018)	0.2770(0.0101)	−0.0293(0.0016)	
500	0.1528(0.0060)	−0.0493(0.0033)	0.1293(0.0096)	−0.0325(0.0029)	
	A_0	B_0	C_0	E_0	F_0
345	(0.2001,0.469)	(−0.3478,0.00140)	(0.0479,0.3276)	(0.3823,0.2540)	(−0.2131,0.2260)
500	(0.0738,0.3888)	(0.05995,0.000901)	(0.0608,0.4115)	(0.1522,−0.00798)	(−0.4044,0.1856)

spin observables to be compared directly to our data, which are available as AIP document 033804 [33].

APPENDIX

Suzuki has derived factorized relations between the deuteron spin observables and the isoscalar responses computed in nuclear structure calculations, using the plane wave impulse approximation. Reference [9] used only an *S*-state deuteron, but the effects of the *D* state are included in Ref. [10]. The relations are

$$I_0=(3\alpha^2+2\beta^2+\eta^2-3\varphi^2)\Sigma_0^2+2\varepsilon^2\Sigma_L^2 +(3\gamma^2+2\delta^2+\kappa^2-3\psi^2+2\zeta^2)\Sigma_T^2, \tag{A1}$$

$$I_0A_y=2\mathrm{Re}[(2\alpha-\varphi)\beta^*]\Sigma_0^2+2\mathrm{Re}[(2\gamma-\psi)\delta^*]\Sigma_T^2, \tag{A2}$$

$$I_0A_{yy}=[2\beta^2+\eta^2-6\varphi^2-6\mathrm{Re}(\alpha\varphi^*)]\Sigma_0^2-\varepsilon^2\Sigma_L^2 +[2\delta^2+\kappa^2-\zeta^2-6\psi^2-6\mathrm{Re}(\gamma\psi^*)]\Sigma_T^2, \tag{A3}$$

$$I_0K_y^{y'}=[2\alpha^2+2\beta^2-\eta^2+5\varphi^2-2\mathrm{Re}(\alpha\varphi^*)]\Sigma_0^2 +[2\gamma^2+2\delta^2-\kappa^2+5\psi^2-2\mathrm{Re}(\gamma\psi^*)]\Sigma_T^2, \tag{A4}$$

with $\varphi=(\eta+\zeta)/3$ and $\psi=(\kappa+\lambda)/3$. Here, I_0 is the unpolarized cross section and A_y, A_{yy}, and $K_y^{y'}$ are presented in this work. The isoscalar density, spin-longitudinal, and spin-transverse nuclear responses are defined by

$$\Sigma_0^2=|\langle f\|e^{i\vec{q}\cdot\vec{r}}\|0\rangle|^2 \tag{A5}$$

$$\Sigma_L^2=|\langle f\|\vec{\sigma}\cdot\vec{q}e^{i\vec{q}\cdot\vec{r}}\|0\rangle|^2 \tag{A6}$$

$$\Sigma_T^2=|\langle f\|\vec{\sigma}\times\vec{q}e^{i\vec{q}\cdot\vec{r}}\|0\rangle|^2. \tag{A7}$$

These are to be multiplied by the effective number of nucleons sensed by the deuteron, given by our Glauber calculation as $N_{\mathrm{eff}}=0.74\,A^{0.30}$. The driving terms are the 600 MeV deuteron-nucleon isoscalar t-matrix amplitudes obtained from folding over the deuteron internal wave function [10]

$$\begin{aligned}\alpha&=A_0g_c,\\ \beta&=C_0g_F,\\ \gamma&=C_0g_c,\\ \delta&=B_0g_F,\\ \epsilon&=E_0g_E,\\ \zeta&=F_0g_F,\\ \eta&=3A_0g_Q,\\ \lambda,\mu,\nu,\xi&=0,\\ \kappa&=3C_0g_Q,\end{aligned} \tag{A8}$$

in terms of the isoscalar parts of the *N*-*N* t matrix given below, using the impulse approximation and the four deuteron form factors

$$\begin{aligned}g_C(q)&=8\pi\int j_0(qr/2)[u^2(r)+8w^2(r)]dr,\\ g_Q(q)&=-8\pi\int j_2(qr/2)[u(r)w(r)-w^2(r)]dr,\\ g_S(q)&=8\pi\int j_0(qr/2)[u^2(r)-4w^2(r)]dr,\\ g_L(q)&=-8\pi\int j_2(qr/2)[u(r)w(r)+2w^2(r)]dr,\end{aligned} \tag{A9}$$

with $g_E=g_S+2g_L$ and $g_F=g_S-g_L$. Deuteron wave functions from the Reid [34] and Bonn [35] potentials were used to compute values of these form factors for our momentum transfers of 345 and 500 MeV, as given in Table II. These were compared to the models of Ref. [36,37], and found to be very similar at 345 and 500 MeV/c.

Nucleon-nucleon scattering amplitudes were evaluated using the phase shift parametrization of Arndt *et al.* [21], changing from channel isospins to isoscalar transfer terms as

$$a_0=\frac{1}{4}a_{NP0}+\frac{3}{4}a_{NP1}. \tag{A10}$$

Spin terms used in Eq. (A8) given by Suzuki are related to those used by Arndt *et al.*, who write the Wolfenstein spin decomposition of the *N*-*N* interaction as

$$M = WA + WC(\sigma_{in} + \sigma_{jn}) + WM\sigma_{in}\sigma_{jn} + WG(\sigma_{ip}\sigma_{jp} + \sigma_{iq}\sigma_{jq}) + WH(\sigma_{ip}\sigma_{jp} - \sigma_{iq}\sigma_{jq}). \tag{A11}$$

The relation between the terminologies of Arndt and Suzuki is given by $A = WA$, $B = WM$, $C = WC$, $E = WG - WH$, and $F = WG + WH$. The N-N interactions were obtained from SAID at a nucleon laboratory beam energy of 300 MeV to generate the interactions listed at the centers of our quasifree peaks (12.17° for 345 MeV/c and 17.44° for 500 MeV/c) in Table II. At energy losses away from that for free scattering, these are better evaluated in the ''optimal'' reference frame [38], as has been done to evaluate responses for the (p,n) reaction [1].

With this equipage, computed isoscalar spin responses Σ^2 may be used to generate deuteron spin observables for comparison to our data. The four equations (A1)–(A4) contain four unknowns (I_0, Σ_0, Σ_L, and Σ_T), and we have only three measured quantities A_y, A_{yy}, and $K_y^{y'}$, so no solution is possible to determine the responses. Ratios of responses, such as $R_{LT} = \Sigma_L^2/\Sigma_T^2$ for comparison to the isovector result [1,2], from our data do not give reasonable values, in contrast to the preliminary results shown for one case in Ref. [17]. It appears that the assumptions used for the factorized expressions in Eqs. (A1)–(A4) are not valid for the extraction of nuclear responses in the quasifree region.

Could we have determined the responses if we had measured the absolute scattering cross sections I_0? Equations (A1)–(A4) define four planes in three-dimensional space for the three Σ^2. These intersect at $I_0 = \Sigma_0^2 = \Sigma_L^2 = \Sigma_T^2 = 0$, and therefore nowhere else. The validity of the plane wave impulse approximation leading to these factorized equations must be strongly doubted.

In spite of questions about the means to connect computed nuclear isoscalar spin responses with our data, we can anticipate the application of more sophisticated means to test those responses against our data.

[1] X. Y. Chen *et al.*, Phys. Rev. C **47**, 2159 (1993).
[2] T. N. Taddeucci *et al.*, Phys. Rev. Lett. **73**, 3516 (1994).
[3] P. Barreau *et al.*, Nucl. Phys. **A402**, 515 (1983).
[4] F. Petrovich, J. A. Carr, and H. McManus, Annu. Rev. Nucl. Part. Sci. **36**, 29 (1986).
[5] F. T. Baker *et al.*, Phys. Rep. **632**, 1 (1997).
[6] T. A. Carey, K. W. Jones, J. B. McClelland, J. M. Moss, L. B. Rees, N. Tanaka, and A. D. Bacher, Phys. Rev. Lett. **53**, 144 (1984).
[7] C. Glashausser, K. Jones, F. T. Baker, L. Bimbot, H. Esbensen, R. W. Fergerson, A. Green, S. Nanda, and R. D. Smith, Phys. Rev. Lett. **58**, 2404 (1987).
[8] R. Fergerson, J. McGill, C. Glashausser, K. Jones, S. Nanda, S. Zuxun, M. Bartlett, G. Hoffmann, J. Marshall, and J. McClelland, Phys. Rev. C **38**, 2193 (1988).
[9] T. Suzuki, Prog. Theor. Phys. **86**, 1129 (1990).
[10] T. Suzuki, Nucl. Phys. **A577**, 167c (1994).
[11] M. Morlet *et al.*, Phys. Lett. B **247**, 228 (1990).
[12] M. Morlet *et al.*, Phys. Rev. C **46**, 1008 (1992).
[13] B. N. Johnson *et al.*, Phys. Rev. C **51**, 1726 (1995).
[14] J. Van de Wiele, A. Willis, and M. Morlet, Nucl. Phys. **A588**, 829 (1995).
[15] J. Arvieux, S. D. Baker, A. Boudard, J. Cameron, T. Hasegawa, D. Hutcheon, C. Kerboul, G. Gaillard, and N. V. Sen, Nucl. Instrum. Methods Phys. Res. A **273**, 48 (1988).
[16] M. Froissant and R. Stora, Nucl. Instrum. Methods **7**, 297 (1960).
[17] R. J. Peterson, M. D. Holcomb, M. Morlet, J. Guillot, H. Langevin, L. Rosier, A. Willis, and B. Johnson, Nucl. Phys. **A577**, 161c (1994).
[18] R. R. Whitney, I. Sick, J. R. Ficenic, R. D. Kephart, and W. P. Tower, Phys. Rev. C **9**, 2230 (1974).
[19] B. Quinn *et al.*, Phys. Rev. C **37**, 1609 (1988).
[20] B. Bonin *et al.*, Nucl. Instrum. Methods Phys. Res. A **288**, 379 (1990); **288**, 389 (1990).
[21] R. A. Arndt, L. D. Roper, R. A. Bryan, R. B. Clark, and B. J. VerWest, Phys. Rev. D **28**, 97 (1983).
[22] C. Furget *et al.*, Phys. Rev. C **51**, 1562 (1995).
[23] M. Kirschbach and L. Tiator, Nucl. Phys. **A604**, 385 (1996).
[24] J. Wambach, A. D. Jackson, and J. Speth, Nucl. Phys. **A348**, 221 (1980).
[25] G. Orlandini, M. Traini, and M. Ericson, Phys. Lett. B **179**, 201 (1986).
[26] T. Shigehara, K. Shimuzu, and A. Arima, Nucl. Phys. **A510**, 106 (1990).
[27] A. Fabrocini, Phys. Lett. B **322**, 171 (1994).
[28] R. Cenni and P. Saracco, Nuovo Cimento A **109**, 407 (1996).
[29] R. Rosenfelder, Phys. Lett. **79B**, 15 (1978).
[30] Particle Data Group, Phys. Rev. D **54**, 1 (1996).
[31] J. Ouyang, S. Hoibraten, and R. J. Peterson, Phys. Rev. C **47**, 2809 (1993).
[32] B. L. Clausen, T. Johnson, R. A. Lindgren, K. Kromer, R. J. Peterson, A. D. Bacher, H. Ward and A. L. Williams, Phys. Rev. C **55**, 625 (1997).
[33] See AIP Document No. E-PAPS-PRVCA-57-033804 for values of spin transfer observables across the quasifree peak. E-PAPS document files may be retrieved free of charge from our FTP server (http://www.aip.org/epaps/epaps.htm) or from ftp.aip.org in the directory /epaps/. For further information: e-mail: PAPS@aip.org or fax: 516-576-2223.
[34] R. V. Reid, Ann. Phys. (N.Y.) **50**, 411 (1968).
[35] R. Machleidt, K. Holinde, and Ch. Elster, Phys. Rep. **149**, 1 (1987).
[36] K. Tamura, T. Niwa, T. Sato, and H. Ohtsubo, Nucl. Phys. **A536**, 597 (1992).
[37] P. L. Chung, F. Coester, B. D. Keister, and W. N. Polyzou, Phys. Rev. C **37**, 2000 (1988).
[38] M. Ichimura and K. K. Kawahigashi, Phys. Rev. C **45**, 1822 (1992); **46**, 2117 (1992).